

The SGLT2 Inhibitor Empagliflozin Attenuates Atherosclerosis Progression By Inducing Autophagy

Hualin Xu

Taihe Hospital <https://orcid.org/0000-0002-5767-5063>

Jie Fu

Taihe Hospital

Qiang Tu

Taihe Hospital

Qinyun Shuai

Taihe Hospital

Yizhi Chen

Hubei University of Medicine

Fuyun Wu

Hubei University of Medicine

Zheng Cao (✉ caozheng908@163.com)

Postgraduate Training Basement of Jinzhou Medicinal University

Research

Keywords: Empagliflozin, SGLT2i, Autophagy, Atherosclerosis

Posted Date: October 1st, 2021

DOI: <https://doi.org/10.21203/rs.3.rs-853158/v2>

License:   This work is licensed under a Creative Commons Attribution 4.0 International License.

[Read Full License](#)

Abstract

Background: Cardiovascular disease due to atherosclerosis (AS) is one of the leading causes of death worldwide. Sodium-dependent glucose transporters 2 inhibitor (SGLT2i), empagliflozin (EMPA), is a new type of hypoglycemic drug. Recent studies have shown that EMPA not only reduces increased glucose, but also has cardiovascular protective effects and that it slows the process of AS. However, the underlying mechanism has yet to be defined.

Methods: Male apoE^{-/-} mice were fed a western high-fat diet to establish an AS model. The area and size of atherosclerotic lesions in apoE^{-/-} mice were then assessed by hematoxylin–eosin (HE) staining after EMPA treatment. After EMPA treatment of the mouse macrophage (RAW 264.7), human aortic smooth muscle cells (HASMCs) and human umbilical vein endothelial cells (HUVECs), western blotting was applied to measure the levels of autophagy-related proteins and proinflammatory cytokines. GFP-LC3 puncta were detected by confocal microscopy to confirm autophagosome formation. Oil red staining was performed to detect the foaming of macrophages and HASMCs, flow cytometry was used for cell cycle analysis. EdU, CCK-8 and scratch assays were also performed to examine the cell proliferation and migration of HASMCs.

Results: EMPA suppressed the progression of atherosclerotic lesions in apoE^{-/-} mice. EMPA also induced autophagy in RAW 246.7 cells, HASMCs and HUVECs, and it significantly increased the expression of Beclin1 and the LC3B-II/I ratio. In addition, EMPA decreased the expression of P62 and downregulated the protein levels of inflammatory cytokines, and it inhibited the foaming of RAW 246.7 cells and HASMCs as well as the expression of inflammatory factors via autophagy induction. Furthermore, the results of flow cytometry, EdU assays, CCK-8 cell viability assays and scratch assays indicated that EMPA blocked HASMC proliferation and migration.

Conclusion: EMPA plays an important role in decelerating the progression of AS by inducing autophagy, providing a novel method for anti-AS treatment in the clinic.

Introduction

Atherosclerosis (AS) is the main pathological basis of cardiovascular diseases [1, 2]. AS often occurs in medium and large arteries composed of endothelial cells, vascular smooth muscle cells, macrophages and other vascular cells [3]. AS develops from intimal thickening to fatty streaks and foam cells. Eventually, cholesterol rich fibrous plaques are formed, which narrow or obstruct the arterial lumen and block blood flow.

Sodium-dependent glucose transporters 2 inhibitor (SGLT2i) is new glucose-lowering agents for treatment of type 2 diabetes mellitus (T2DM) and mainly expressed in the S1 and S2 segments of the renal proximal tubule [4]. SGLT2 is responsible for approximately 90% of renal glucose reabsorption in the kidney, and SGLT2i plays a hypoglycemic role by inhibiting glucose reabsorption in renal proximal convoluted tubules [5, 6]. At present, empagliflozin (EMPA) is one of the three SGLT-2i approved in the

United States. Recent studies have shown that SGLT2i protects against atherosclerotic cardiovascular disease (ASCVD), and reduces heart failure (HF) hospitalization and cardiovascular mortality [7–10]. Furthermore, recent studies have shown that EMPA induces SIRT1/AMPK and Akt/mTOR signal transduction pathways to influence autophagy and that it may influence the process of diabetic cardiomyopathy, myocardial infarction, fatty liver and other diseases through autophagy [11–13].

Because studies have reported that autophagy is one of the important mechanisms regulating AS [14], it is thoroughly explored in the present study. Recent evidence shows that autophagy plays an important role in regulating the formation of AS and the stability of atherosclerotic plaques. Three categories of cells, namely, macrophages, smooth muscle cells and vascular endothelial cells, are relevant for the occurrence and development of AS. First, autophagy promotes cholesterol efflux from macrophage foam cells in atherosclerotic lesions, inhibits the formation of macrophage foam cells and can promote the stability of atherosclerotic plaques by protecting cells and reducing the secretion of inflammatory factors [15, 16]. Second, impaired autophagy of endothelial cell responses may cause endothelial dysfunction and dramatically enhance the expression of proinflammatory cytokines (TNF- α and IL-6), resulting in atherosclerotic thrombosis [17, 18]. For SMCs, enhanced autophagy inhibits free cholesterol from entering SMCs, which blocks the formation of SMC-derived foam cells, thereby inhibiting cell death and slowing the progression of AS [19]. Therefore, moderate autophagy of these three cell types may help to preserve normal cellular functions to maintain the stability of plaques and exert an antiatherosclerotic effect.

Both SGLT2i and autophagy can have a protective effect on AS, and studies have shown that SGLT2i also interact with autophagy. However, it remains unknown whether SGLT2i delays the process of AS through autophagy. Through WB, GFP-LC3 puncta assay, Oil Red O staining, H&E staining and other assays, the present study demonstrated that SGLT2i slows AS progression by promoting autophagy, thereby providing a new strategy for the clinical treatment of AS.

Materials And Methods

Chemicals, Reagents, and Antibodies

EMPA and 3-methyladenine (3-MA) (purity > 98%) were purchased from MedChemExpress (MCE, Shanghai, China). The anti-GAPDH antibody (10494-1-AP), anti-SQSTM1/P62 antibody (18420-1-AP), anti-LC3B antibody (18725-1-AP), anti-Beclin1 antibody (11306-1-AP), anti-IL-6 antibody (66146-1-Ig) and anti-TNF- α antibody (60291-1-Ig) were purchased from Proteintech Group, Inc. Human oxidized low density lipoprotein (oxLDL) and Oil Red O staining solutions were purchased from Yiyuan Biotechnologies (Guangzhou, China). The CCK-8 kit, cell cycle apoptosis kit and antibody diluent were obtained from Beyotime Biotechnology (Shanghai, China). The KeyFlour 488 Click-iT EdU imaging detection kit was obtained from KEYGEN Biotech (Nanjing, China). The HRP-conjugated secondary antibodies, goat-anti-mouse secondary antibody and goat-anti-rabbit secondary antibody were purchased from Beyotime Biotechnology (Shanghai, China).

Animals

Male C57BL/6J and ApoE^{-/-} mice (8 weeks old) were purchased from Beijing Huaifukang Biotechnology Co., Ltd. (Beijing, China), and ApoE^{-/-} mice were used to establish animal models of AS. All in vivo experiments followed the ARRIVE guidelines [20]. ApoE^{-/-} mice were fed a high-fat diet (containing 21% fat and 0.15% cholesterol) for 8 weeks to induce AS. After 8 weeks of modeling, different doses of EMPA (1.5 and 3.5 mg/kg/d) were injected intraperitoneally for 8 weeks. After 8 weeks, samples were collected for the follow-up test, and mice were randomly divided into the following four groups (n = 6 mice per group): blank control group (C57BL/6J), model control group (DMSO), low-dose group (1.5 mg/kg/d; EMPA) and high-dose group (3.5 mg/kg/d; EMPA). To avoid the potential confounding effects of dietary differences between different batches, we retained and used a single batch of diets.

H&E Staining

The three parts of the aortic arch, thorax and abdomen of C57BL/6J- mice and ApoE^{-/-} mice were collected, fixed for 24 hours, embedded in paraffin and sectioned. The paraffin sections were dewaxed in water, and nuclei were stained with hematoxylin. The sections were then stained with eosin staining solution for 1–3 minutes, dehydrated, mounted with neutral gum and observed under a microscope.

Cell Culture

The mouse macrophage (RAW 264.7) and RAW 264.7 cell complete culture medium were purchased from Procell Life Science & Technology Co. Ltd. (Shanghai, China). Human vein endothelial cells (HUVECs) were obtained from Icell Bioscience Inc. (Shanghai, China) and cultured in an endothelial cell culture system containing 93% endothelial cell culture medium, 5% fetal bovine serum (FBS), 1% P/S and 1% endothelial cell culture additive. Human aortic smooth muscle cells (HASMCs)(CL-0517) were obtained from Procell Life Science & Technology Co. Ltd. (Shanghai, China) and cultured in DMEM supplemented with 10% FBS (HyClone) and 1% P/S. All cells were cultured in a humid air incubator containing 5% CO₂ at 37°C, and after culturing to 80–90% confluence, they were passaged, frozen or used for experiments.

Cell Transfection

A GFP-LC3 plasmid (2.5 µg/ml, Genomeditech (Shanghai) Co., Ltd., Shanghai, China) was transfected into RAW 264.7 cells, HASMCs and HUVECs with Lipofetamine®8000 (Invitrogen; Thermo Fisher Science, Inc.) for 24–48 h and then incubated with oxLDL (80 µg/mL) and EMPA (50 µM) at 37°C for 24 h. Finally, autophagosomes were observed under a laser confocal microscope.

Western Blot Analysis

After cell treatment, cells were lysed, and total protein was extracted. The protein concentration was measured by the BCA method. Protein samples were separated by SDS–PAGE, transferred to PVDF membranes and blocked with 5% skim milk for 2 h. Then incubated with primary antibodies overnight at 4°C. Subsequently, the membranes were incubated with horseradish peroxidase (HRP)-conjugated

secondary antibody for 2 h at room temperature and detected with an enhanced chemiluminescence system. Relative target protein expression levels were calculated using Image Lab software (Bio–Rad Laboratories, Inc.).

Oil Red O Staining

Cells were seeded into a 6-well plate, treated with oxLDL (80 µg/ml) for 24 h, pretreated with different doses of EMPA (30 and 50 µM) in DMEM containing 10% fetal calf serum for 24 h and washed three times with PBS. Subsequently, cells were fixed with paraformaldehyde at 37°C for 30 minutes, stained with Oil Red O staining solution at 37°C for 20 minutes and rinsed with 60% isopropanol for 10 seconds. After quickly washing twice with PBS, the accumulation of lipids in macrophages was observed under an inverted microscope (Nikon Ti-S, Japan).

Cell Viability Assay

Cell viability assays were performed using the Cell Counting Kit-8 (CCK8). HASMCs were cultured in 96-well plates (1×10^4 cells/well) for 24 h. Cells were then treated with different concentrations of EMPA (10,30,50 and 100 µM) for 24 h. After treatment, 10 µl of CCK8 solution was added to each well at 37°C for 1 hour, and the absorbance values at 450 nm were then measured with spectroscopy (µQuant spectrophotometer, Bio-Tek Instruments, Winooski, VT).

Cell Cycle Analysis

HASMCs were cultured with different concentrations of EMPA for 24 h, and cells were then collected and washed with PBS precooled at 4 °C. The supernatant was removed by centrifugation at 1000 g and incubated overnight in 70% ethanol at 4 °C. The supernatant was discarded and then resuspended in PBS precooled at 4 °C on the second day. After centrifugation, the supernatant was discarded and treated with propidium iodide (50 µg/ml) and ribonuclease A (100 µg/ml) for 30 min. DNA fluorescence was detected by a Beckman Coulter CyAn ADP cell analyzer (Brea, CA). Flow cytometry data were evaluated with ModFit software (ModFit wintrial).

EdU Staining

HASMCs were counted and seeding into 24-well plates (2×10^4 cells/well). When the cell density reached 70%-80%, different concentrations of EMPA (50 and 100 µM) were added followed by incubation for 24 hours. EdU reagent was then added into the medium for a final concentration of 100 µM, and cells were incubated for an additional 24 h. Cells were then fixed, processed according to the instructions of the Fluor 488 EdU cell proliferation detection kit and stained with DAPI. Finally, cells were observed under a fluorescence microscope.

Scratch Assay

HASMC migration was evaluated by a scratch assay[21]. HASMCs were plated into 6-well plates. A 20 µl Axygen pipet tip was used to make a scratch in the cell monolayer after cells had grown to 90% confluence, and floating cells in each well were washed away twice using PBS. After adding culture

medium, cells were treated with different concentrations of EMPA (0, 50 and 100 μ M) for 24 hours in a 5% CO₂ incubator at 37 °C. Images of scratches were acquired at the beginning of the experiment and 24 hours later.

Statistical Analysis

All data represent at least three independent experiments and are expressed as mean \pm standard deviation. The paired-sample t test was used to compare the differences between the two groups. All statistical analyses were performed using Prism 8 (GraphPad Software, San Diego, USA). * $P < 0.05$ is considered a statistically significant difference.

Results

EMPA stabilizes the established AS in ApoE $-/-$ mice

To evaluate the therapeutic role of EMPA in AS in mice, we employed ApoE $-/-$ mice to generate an in vivo model of AS. The aortic arch, thorax and abdomen of the four groups were processed for H&E staining. According to the staining results shown in Fig. 1, the atherosclerotic plaque lesion size of ApoE $-/-$ mice in the EMPA group was significantly smaller than that in the control group. The higher dose of EMPA had a more profound affect than the lower dose. These findings indicated that EMPA stabilizes established atherosclerotic plaques in apoE $-/-$ mice.

EMPA inhibits oxLDL-induced formation of foam cells and decreases the synthesis of proinflammatory cytokines by promoting autophagy in the RAW 246.7 cells

The formation of macrophage-derived foam cells is a critical step in the development of AS [22]. To identify the effects of EMPA on lipid accumulation, RAW264.7 cells were treated with oxLDL (80 μ g/mL) for 24 h. In RAW 264.7 cells, the presence of Oil Red O staining increased in the oxLDL group, but the amount of lipid accumulation in the EMPA group was significantly reduced compared to the oxLDL group (Fig. 2A), suggesting that EMPA inhibits the formation of oxLDL-induced macrophage-derived foam cells. To further clarify the mechanism by which EMPA affects the progression of AS, we analyzed the effect of EMPA on autophagosomes using a GFP-LC3 puncta assay. oxLDL treatment (80 μ g/ml) for 24 h followed by incubation with EMPA (50 μ M) increased the GFP-LC3 green fluorescent puncta in the cytoplasm of RAW 264.7 cells (Fig. 2B, C). Western blotting was also used to detect the levels of autophagy-related proteins in RAW 264.7 cells. After treatment of RAW 264.7 cells with EMPA for 24 hours, the expression levels of Beclin1 was increased, LC3B-II/I ratio was also augmented, and the expression of P62 decreased (Fig. 2D-G). These results suggested that EMPA may induce autophagy in RAW 246.7 cells. We next investigated the effect of 3MA as shown in Fig. 2F-I. Compared to the EMPA group, Oil Red O staining was significantly increased in the 3MA group, and western blot analysis demonstrated that the

expression level of inflammatory factors in the 3MA group was also significantly increased. These results demonstrated that EMPA inhibits the formation of macrophage foam cells and the expression of inflammatory factors via autophagy induction in RAW 264.7 cells, thus playing an antiatherosclerotic role.

EMPA Hinders the OxLDL-induced Inflammatory Response in HUVECs by Inducing Autophagy in HUVECs

Endothelial dysfunction is the key cause of AS. Endothelial dysfunction can cause lipid accumulation, inflammation and AS. Therefore, the reduction in proinflammatory cytokine synthesis reflects the effect of EMPA on AS [23]. As depicted in Fig. 3A and C, the expression of proinflammatory cytokines (TNF- α and IL-6) in the EMPA group was significantly reduced compared to that in the oxLDL group.

To further explore the mechanism by which EMPA affects inflammatory factors, we used western blot analysis and green fluorescent puncta experiments. There were more green fluorescent puncta in the EMPA group compared to the oxLDL group. Compared to the oxLDL group, western blot analysis showed that the protein expression of LC3B was significantly increased in the EMPA group, while the protein expression of P62 was decreased in the EMPA group (Fig. 3A, B, D, E). These findings showed that EMPA promotes autophagy in HUVECs. To explore whether EMPA affects the expression of proinflammatory cytokines in HUVECs through autophagy induction, we treated HUVECs with 3MA. Western blot analysis demonstrated that the expression of proinflammatory cytokines was increased after treatment with 3MA (Fig. 3A, C), suggesting that EMPA inhibits the oxLDL-induced inflammatory response in HUVECs by inducing autophagy.

EMPA inhibits the formation of HASMC-derived foam cells induced by OxLDL by promoting autophagy and inhibiting the proliferation and migration of HASMCs

Smooth muscle cells are an important source of foam cells. To explore the effect of EMPA on lipid accumulation in HASMCs, Oil Red O staining experiments were performed. Compared to the blank control group, Oil Red O staining was significantly increased in the oxLDL group, and treatment of HASMCs with EMPA significantly reduced the lipid accumulation compared to the oxLDL group (Fig. 4A). These results suggested that EMPA reduces the oxLDL-induced lipid accumulation, indicating that EMPA may have an inhibitory effect on the lipid accumulation of HASMCs.

To further clarify whether EMPA affects the autophagy of HASMCs and whether it inhibits the foaming of HASMCs by inducing autophagy, we transfected GFP-LC3 into cells and observed the number of autophagosomes. The protein expression of autophagy-related proteins was also determined by western blot analysis. Similar results were obtained, indicating that EMPA promoted autophagy in HASMCs (Fig. 4B-E). Moreover, the autophagy inhibitor, 3MA, weakened the effect of EMPA in inhibiting the foaming of

HASMCs (Fig. 4F). The above results indicated that EMPA inhibits oxLDL-induced HASMC foam cell formation by promoting autophagy.

Because the proliferation and migration of HASMCs accelerate the process of AS [24], we tested the effect of EMPA on the proliferation and migration of HASMCs. The CCK-8 cell viability assay indicated that treatment of HASMCs with EMPA for 24 h resulted in inhibition of cell proliferation (Fig. 5A). Similarly, the EdU experiment demonstrated that the proportion of proliferating cells was significantly reduced after HASMCs were treated with EMPA (Fig. 5B,C). Subsequently, the effect of EMPA on cell cycle progression was investigated. The addition of EMPA (50 and 100 μ M) blocked HASMCs in the G0/G1 phase of the cell cycle as indicated by an increase in the proportion of cells in the G0/G1 phase and a decrease in the proportion of cells in the S phase, indicating that EMPA inhibits HASMC DNA synthesis (Fig. 5D, E). Using scratch assays, we further tested the effect of EMPA on the migration of HASMCs. The results showed that the healing rate of cell scratches was slower than that of the control group after EMPA treatment (Fig. 5F, G). The above results indicated that EMPA inhibits the foaming of HASMCs via autophagy induction as well as the proliferation and migration of HASMCs.

Discussion

AS is a chronic inflammatory disease of large and middle arteries. Proinflammatory cytokines (TNF- α and IL-6) affect the occurrence, progression and complications of AS [25], and AS is also a progressive disease. Vascular endothelial cell dysfunction, macrophage-derived foam cell formation, smooth muscle cell-derived foam cell formation, smooth muscle cell migration and smooth muscle cell proliferation result in loss of vascular homeostasis. OxLDL plays a prominent role in the formation of atherosclerotic lesions. Macrophages and smooth muscle cells recognize and internalize the excess lipids of oxLDL through scavenger receptors to form foam cells, and the accumulation of foam cells to form lipid streaks and even atherosclerotic plaques is the key pathological link in the early stage of AS [26].

Cardiovascular disease caused by atherosclerosis is the leading cause of death worldwide, but its specific molecular mechanism has not yet been fully elucidated. Recently, several studies have shown that autophagy plays an important role in regulating the formation of AS and the stability of atherosclerotic plaques,, potentially providing new opportunities for the treatment of AS [27–29]

EMPA is a new type of SGLT2 inhibitor for the treatment of type 2 diabetes. A recent study has shown that EMPA not only has a hypoglycemic effect but also exhibits cardiovascular protection, but the specific mechanism is not yet clear, and needs further experimental validation [30] .

The present study demonstrated that EMPA had antiatherosclerotic effects in atherosclerosis model mice. In addition, EMPA induced autophagy in RAW 264.7 cells, HUVECs and HASMCs. EMPA inhibited oxLDL-induced foaming of RAW 264.7 cells and HASMCs by inducing autophagy. In addition, EMPA hindered the inflammatory response of RAW 264.7 cells and HUVECs by inducing autophagy. Further, EMPA inhibited the proliferation and migration of HASMCs (Fig. 6).

As a new type of hypoglycemic agent, EMPA inhibits the SGLT-2 receptor in renal tubular epithelial cells and inhibits the reabsorption of glucose to exert a hypoglycemic effect. The present study found SGLT-2 receptors in RAW 264.7 cells, HUVECs and HASMCs, suggesting that EMPA might induce autophagy by inhibiting the glucose uptake of these three cell types. Therefore, the SGLT-2 receptor may be a potential new target for the treatment of AS, and EMPA is also expected to be an effective drug for the treatment of atherosclerosis.

Overall, EMPA delays the occurrence and development of atherosclerosis by promoting autophagy. This study reveals the potential medicinal value of EMPA in the treatment of AS, which is of great significance for the clinical treatment of atherosclerosis.

Conclusion

In summary,our results not only indicated that EMPA can play an anti-atherosclerotic effect by promoting autophagy to delay the occurrence and development of AS, but also provides a rationale for use of EMPA in clinical treatment of AS.

Abbreviations

AS: Atherosclerosis; SGLT2i: Sodium-dependent glucose transporters 2 inhibitor; EMPA: empagliflozin; HE:hematoxylin–eosin;T2DM:type 2 diabetes mellitus; HRP: horseradish peroxidase; RAW 264.7: The mouse macrophage; HASMCs:human aortic smooth muscle cells; HUVECs:human umbilical vein endothelial cells; oxLDL: Human oxidized low density lipoprotein.

Declarations

Acknowledgments

None

Fundings

This study was financially supported by the National Natural Science Foundation of China (NO.81771522) , Hubei Provincial Health Commission Project (NO.WJ2021M258) and Cultivating Project for Young Scholar at Hubei University of Medicine(Grant No.2020QDJZR026).

Authors' contributions

HLX performed the experiment, data analysis, prepared the figures and wrote the manuscript. JF, QT, QYS and YZC provided support with experimental techniques and performed data analysis. ZC and FYW conceived the study, designed the experiments and helped with data analysis. All authors read and approved the final manuscript.

Availability of data and materials

All data and materials involved in this work are available.

Ethics approval and consent to participate

This experiment was approved by the Animal Management Committee of Hubei Medical College in accordance with the Animal Laboratory Animal Guidelines of Hubei Medical College and strictly abide by the rules of the Experimental Animal Ethics Committee of Hubei Medical College.

Consent for publication

Not applicable.

Conflict of interest

The authors declared that they have no competing interests.

Author details

¹Postgraduate Training Basement of Jinzhou Medicical University, Taihe Hospital, Hubei University of Medicine, Shiyan 442000, China. ²Department of Cardiology, Taihe Hospital, Hubei University of Medicine, Shiyan 442000, Hubei, China. ³School of Basic Medical Sciences, Hubei University of Medicine, Shiyan 442000, Hubei, China.

References

1. Aviram M. Atherosclerosis: cell biology and lipoproteins–inflammation and oxidative stress in atherogenesis: protective role for paraoxonases. *Curr Opin Lipidol*. 2011;22:243–4.
2. Scannapieco FA, Bush RB, Paju S. Associations between periodontal disease and risk for atherosclerosis, cardiovascular disease, and stroke. A systematic review. *Ann Periodontol*. 2003;8:38–53.
3. Kasikara C, Doran AC, Cai B, Tabas I. The role of non-resolving inflammation in atherosclerosis. *J Clin Invest*. 2018;128:2713–23.
4. Okamoto A, Yokokawa H, Sanada H, Naito T. Changes in Levels of Biomarkers Associated with Adipocyte Function and Insulin and Glucagon Kinetics During Treatment with Dapagliflozin Among Obese Type 2 Diabetes Mellitus Patients. *Drugs R D*. 2016;16:255–61.
5. Wright EM. Renal Na(+)-glucose cotransporters. *Am J Physiol Renal Physiol*. 2001;280:F10–8.
6. Wright EM, Turk E. The sodium/glucose cotransport family SLC5. *Pflugers Arch*. 2004;447:510–8.
7. Zelniker TA, Braunwald E. Cardiac and Renal Effects of Sodium-Glucose Co-Transporter 2 Inhibitors in Diabetes: JACC State-of-the-Art Review. *J Am Coll Cardiol*. 2018;72:1845–55.

8. Arnott C, Li Q, Kang A, Neuen BL, Bompont S, Lam CSP, Rodgers A, Mahaffey KW, Cannon CP, Perkovic V, et al. Sodium-Glucose Cotransporter 2 Inhibition for the Prevention of Cardiovascular Events in Patients With Type 2 Diabetes Mellitus: A Systematic Review and Meta-Analysis. *J Am Heart Assoc.* 2020;9:e014908.
9. Fei Y, Tsoi MF, Cheung BM. Cardiovascular outcomes in trials of new antidiabetic drug classes: a network meta-analysis. *Cardiovasc Diabetol.* 2019;18:112.
10. Levine MJ. Empagliflozin for Type 2 Diabetes Mellitus: An Overview of Phase 3 Clinical Trials. *Curr Diabetes Rev.* 2017;13:405–23.
11. Packer M. SGLT2 Inhibitors Produce Cardiorenal Benefits by Promoting Adaptive Cellular Reprogramming to Induce a State of Fasting Mimicry: A Paradigm Shift in Understanding Their Mechanism of Action. *Diabetes Care.* 2020;43:508–11.
12. Nasiri-Ansari N, Nikolopoulou C, Papoutsis K, Kyrou I, Mantzoros CS, Kyriakopoulos G, Chatzigeorgiou A, Kalotychou V, Randeve MS, Chatha K, et al: **Empagliflozin Attenuates Non-Alcoholic Fatty Liver Disease (NAFLD) in High Fat Diet Fed ApoE((-/-)) Mice by Activating Autophagy and Reducing ER Stress and Apoptosis.** *Int J Mol Sci* 2021, 22.
13. Jiang K, Xu Y, Wang D, Chen F, Tu Z, Qian J, Xu S, Xu Y, Hwa J, Li J, et al: **Cardioprotective mechanism of SGLT2 inhibitor against myocardial infarction is through reduction of autosis.** *Protein Cell* 2021.
14. Tian J, Popal MS, Liu Y, Gao R, Lyu S, Chen K, Liu Y. Ginkgo Biloba Leaf Extract Attenuates Atherosclerosis in Streptozotocin-Induced Diabetic ApoE^{-/-} Mice by Inhibiting Endoplasmic Reticulum Stress via Restoration of Autophagy through the mTOR Signaling Pathway. *Oxid Med Cell Longev.* 2019;2019:8134678.
15. Shao BZ, Han BZ, Zeng YX, Su DF, Liu C. The roles of macrophage autophagy in atherosclerosis. *Acta Pharmacol Sin.* 2016;37:150–6.
16. Zhai C, Cheng J, Mujahid H, Wang H, Kong J, Yin Y, Li J, Zhang Y, Ji X, Chen W. Selective inhibition of PI3K/Akt/mTOR signaling pathway regulates autophagy of macrophage and vulnerability of atherosclerotic plaque. *PLoS One.* 2014;9:e90563.
17. De Meyer GR, Grootaert MO, Michiels CF, Kurdi A, Schrijvers DM, Martinet W. Autophagy in vascular disease. *Circ Res.* 2015;116:468–79.
18. Shadab M, Millar MW, Slavin SA, Leonard A, Fazal F, Rahman A. Autophagy protein ATG7 is a critical regulator of endothelial cell inflammation and permeability. *Sci Rep.* 2020;10:13708.
19. Xu K, Yang Y, Yan M, Zhan J, Fu X, Zheng X. Autophagy plays a protective role in free cholesterol overload-induced death of smooth muscle cells. *J Lipid Res.* 2010;51:2581–90.
20. Kilkenny C, Browne WJ, Cuthill IC, Emerson M, Altman DG. Improving bioscience research reporting: the ARRIVE guidelines for reporting animal research. *PLoS Biol.* 2010;8:e1000412.
21. Peyton KJ, Yu Y, Yates B, Shebib AR, Liu XM, Wang H, Durante W. Compound C inhibits vascular smooth muscle cell proliferation and migration in an AMP-activated protein kinase-independent fashion. *J Pharmacol Exp Ther.* 2011;338:476–84.

22. Cai J, Zhang M, Liu Y, Li H, Shang L, Xu T, Chen Z, Wang F, Qiao T, Li K. Iron accumulation in macrophages promotes the formation of foam cells and development of atherosclerosis. *Cell Biosci.* 2020;10:137.
23. Menghini R, Casagrande V, Marino A, Marchetti V, Cardellini M, Stoeckl R, Rizza S, Martelli E, Greco S, Mauriello A, et al. MiR-216a: a link between endothelial dysfunction and autophagy. *Cell Death Dis.* 2014;5:e1029.
24. Behnammanesh G, Durante GL, Khanna YP, Peyton KJ, Durante W. Canagliflozin inhibits vascular smooth muscle cell proliferation and migration: Role of heme oxygenase-1. *Redox Biol.* 2020;32:101527.
25. Wu M, Yang S, Wang S, Cao Y, Zhao R, Li X, Xing Y, Liu L. Effect of Berberine on Atherosclerosis and Gut Microbiota Modulation and Their Correlation in High-Fat Diet-Fed ApoE^{-/-} Mice. *Front Pharmacol.* 2020;11:223.
26. Di Pietro N, Formoso G, Pandolfi A. Physiology and pathophysiology of oxLDL uptake by vascular wall cells in atherosclerosis. *Vascul Pharmacol.* 2016;84:1–7.
27. Schrijvers DM, De Meyer GR, Martinet W. Autophagy in atherosclerosis: a potential drug target for plaque stabilization. *Arterioscler Thromb Vasc Biol.* 2011;31:2787–91.
28. Mewton N, Thibault H, Roubille F, Lairez O, Rioufol G, Sportouch C, Sanchez I, Bergerot C, Cung TT, Finet G, et al. Postconditioning attenuates no-reflow in STEMI patients. *Basic Res Cardiol.* 2013;108:383.
29. Martinet W, De Loof H, De Meyer GRY. mTOR inhibition: a promising strategy for stabilization of atherosclerotic plaques. *Atherosclerosis.* 2014;233:601–7.
30. Ndefo UA, Anidiobi NO, Basheer E, Eaton AT. Empagliflozin (Jardiance): A Novel SGLT2 Inhibitor for the Treatment of Type-2 Diabetes. *P t.* 2015;40:364–8.

Figures

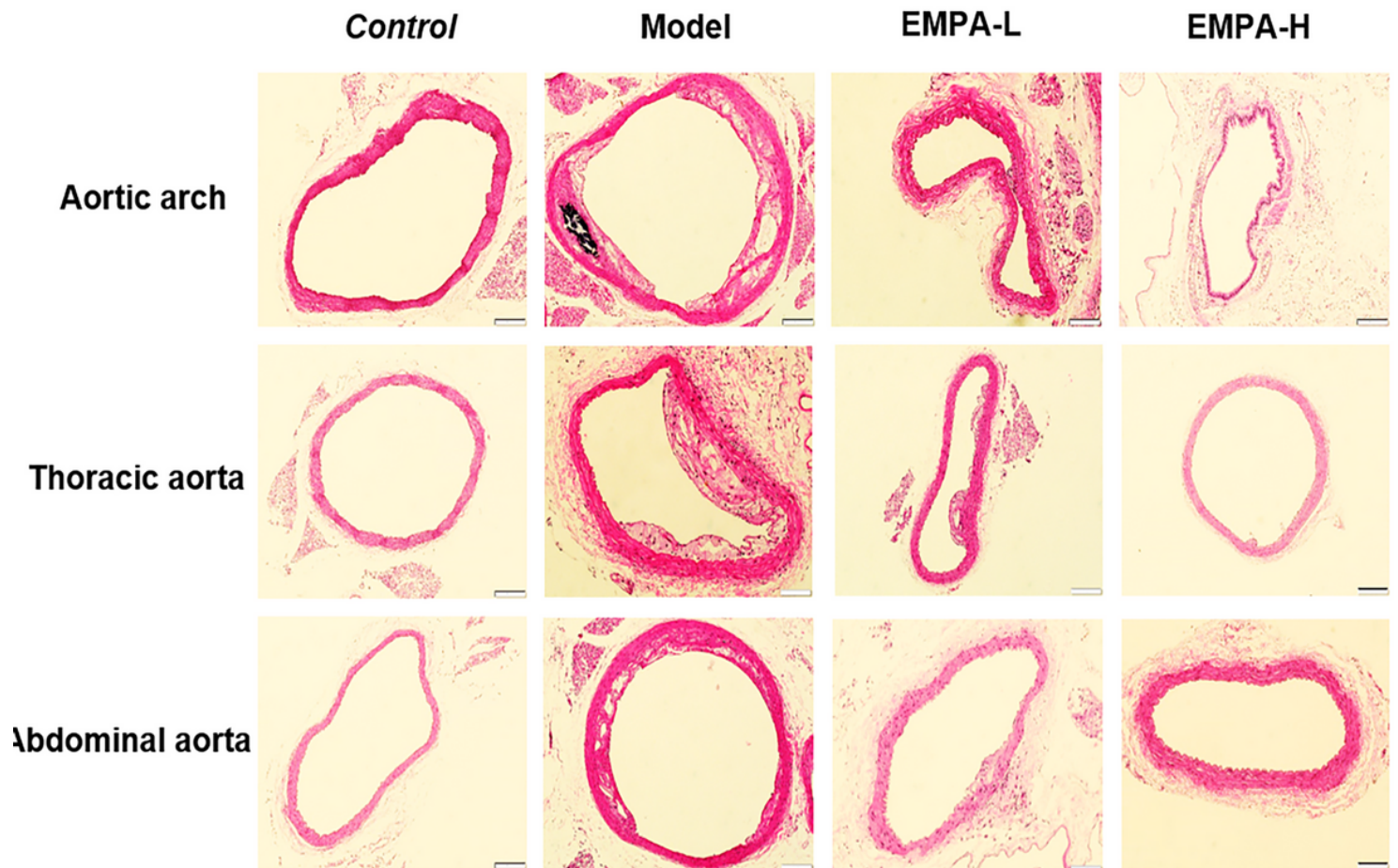


Figure 1

H&E staining for aorta structure (n=6), control: the aort of male C57BL/6J; Model: the aort of apoE^{-/-} mice, EMPA-L: the aort of apoE^{-/-} mice treated with low dose of EMPA (1.5 mg/kg/d), EMPA-H: the aort of apoE^{-/-} mice treated with high dose of EMPA (3.5 mg/kg/d), Scale bar =20 μ m.

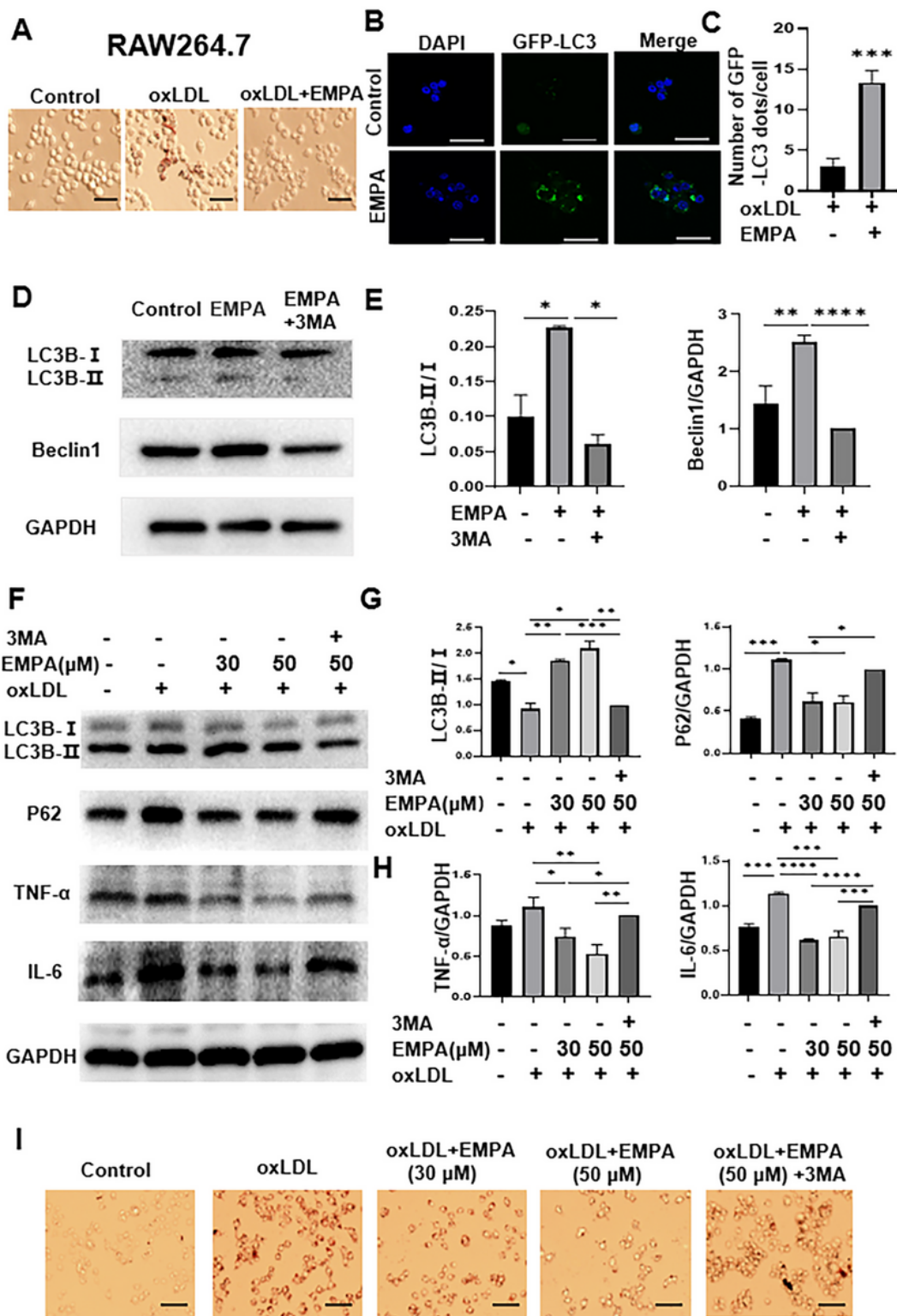


Figure 2

EMPA hindered macrophage-derived foam cell formation through autophagy induction (a)(i) Oil red staining to detect changes in cytoplasmic lipids. Scale bars=20 μm. (b) The green puncta images of RAW 264.7 cells were captured using a confocal microscope (Leica). Scale bar=5 μm.(c) Quantitative analysis of GFP-tagged LC3 puncta per cell (d,e) Protein expression of LC3B and Beclin1 in RAW 264.7 cells.(f-h)

Protein expression of LC3B,P62,TNF-α and IL-6 in RAW 264.7 cells. *P≤0.05,** P≤0.01,***P≤0.001,****P≤0.0001. Results were presented as mean ± S.D. (error bars) of three independent experiments.

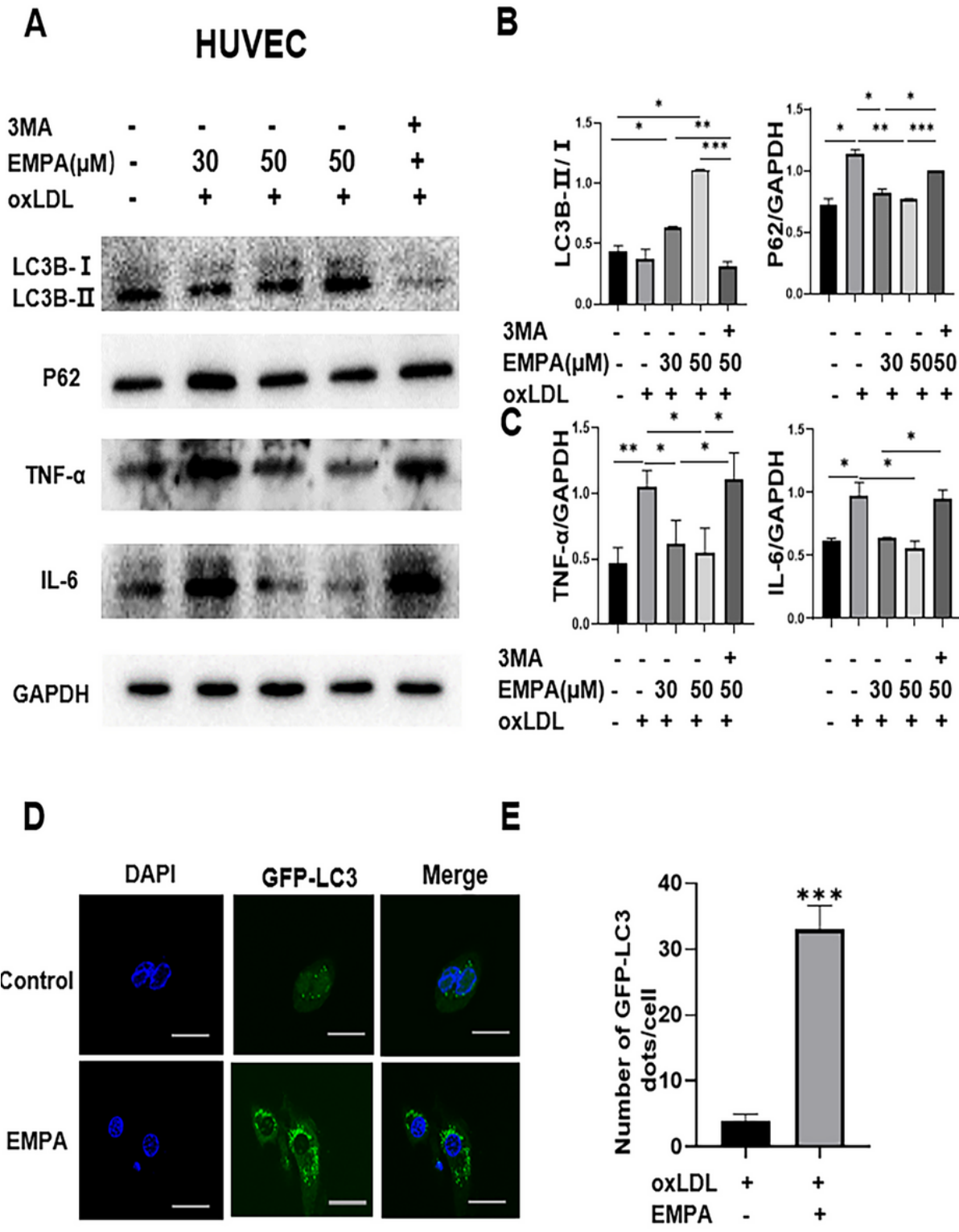


Figure 3

EMPA inhibited inflammatory response in HUVECs through autophagy induction(a-c) Protein expression of LC3B, P62,TNF-α and IL-6 in HUVECs.(d)The green puncta images in HUVECs were captured using a confocal microscope (Leica).(e) Quantitative analysis of GFP-tagged LC3 puncta per cell. Scale bar=5

μm. *P<0.05,** P<0.01, ***P<0.001,****P<0.0001. Results were presented as mean±S.D. (error bars) of three independent experiments.

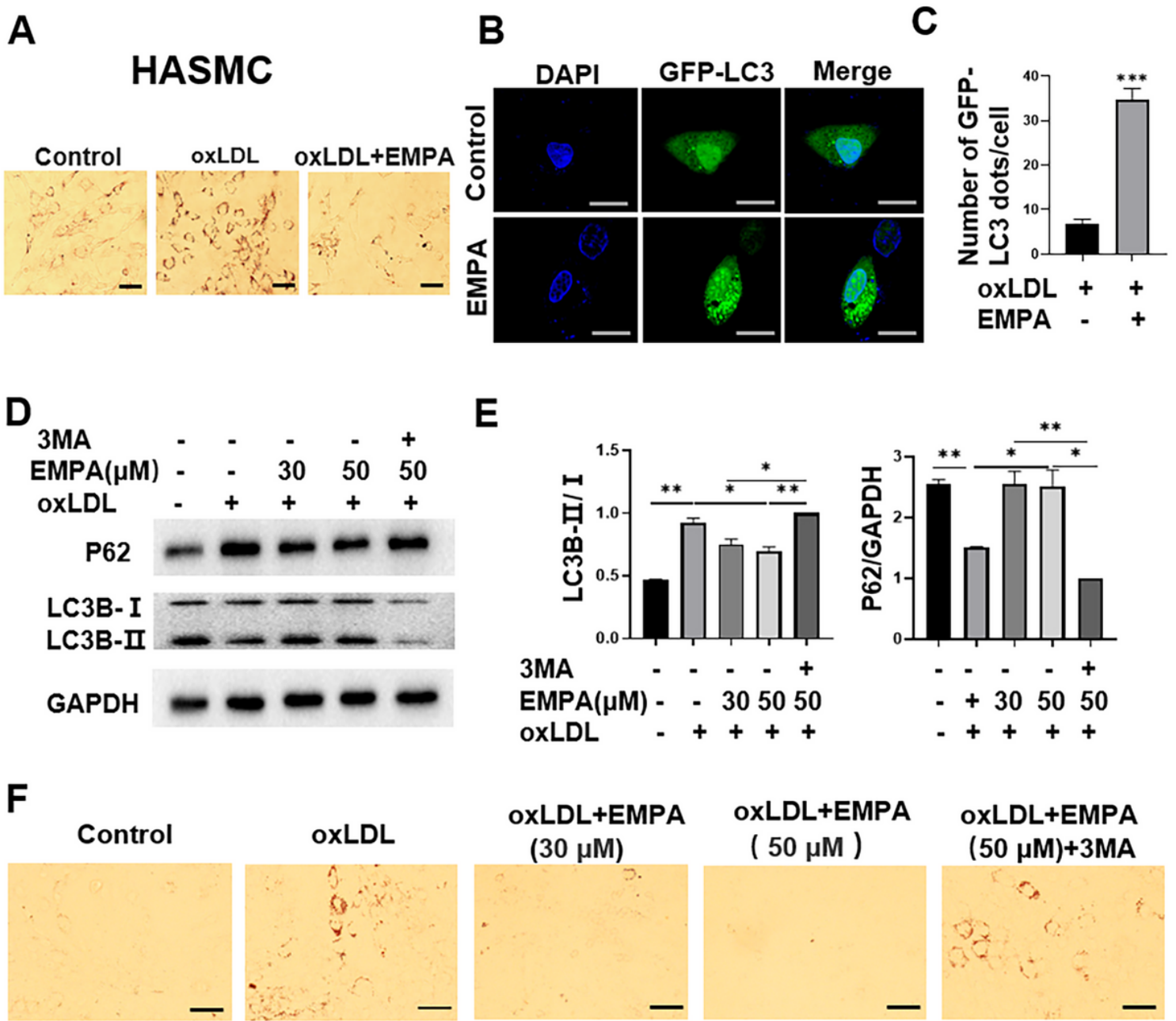


Figure 4

EMPA inhibited HASMC-derived foam cell formation through autophagy induction(a)(f) Oil red staining.Scale bars = 20 μm. (b) The green puncta images in HUVECs were captured using a confocal microscope (Leica). Scale bar=5 μm. (c) Quantitative analysis of GFP-tagged LC3 puncta per cell. (d,e) Protein expression of LC3B, P62.*P<0.05,** P<0.01, ***P<0.001,****P<0.0001. Results were presented as mean±S.D. (error bars) of three independent experiments.

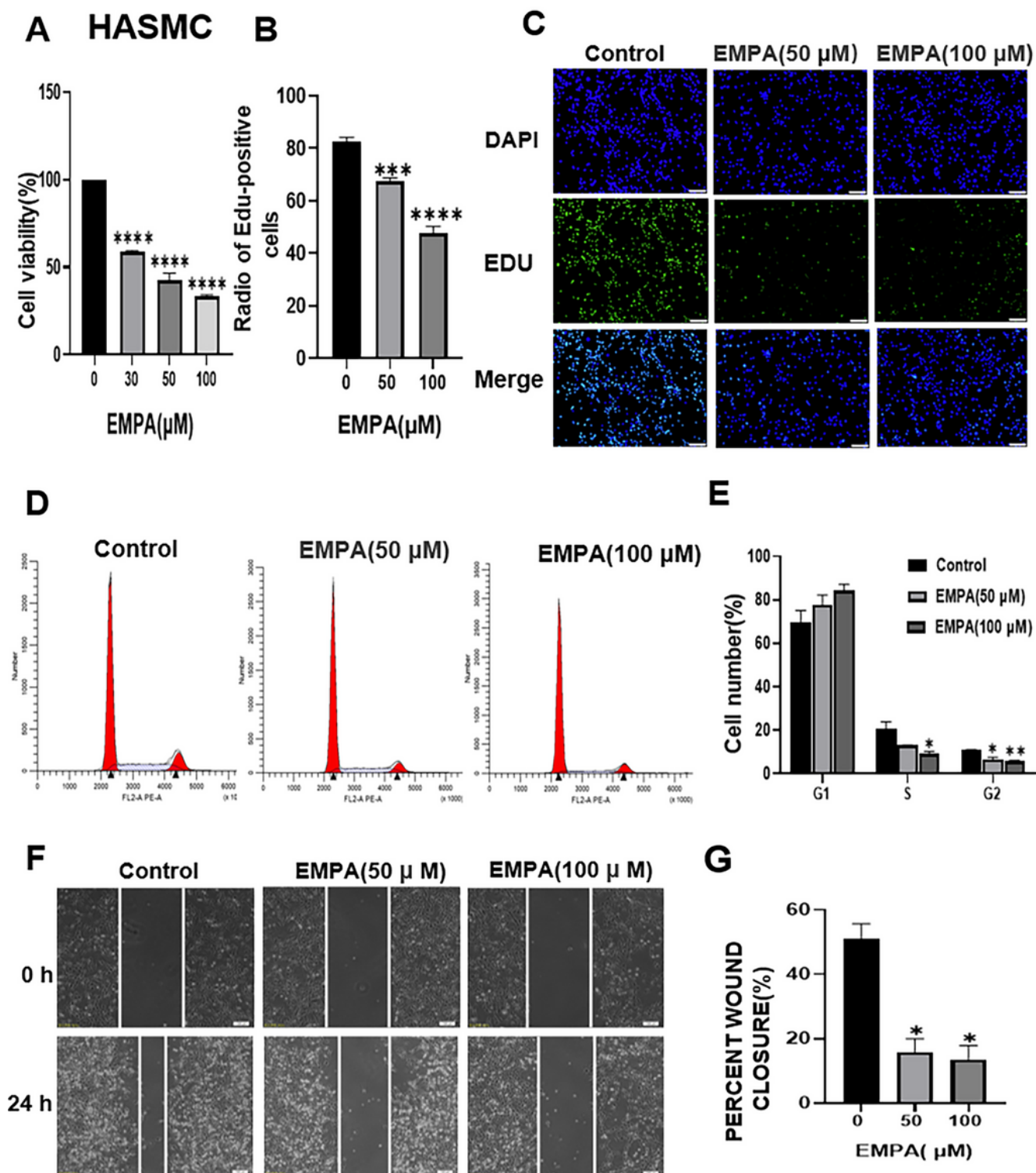


Figure 5

EMPA prevented the proliferation and migration of HASMCs. (a) CCK8 assay for cell viability. (b,c) Detection of cell proliferation by kfluor488 EDU Staining, Scale bars=1 mm. (d,e) Cell cycle analysis.(f,g) Scratch assay, Scale bars=100 μm. * $P \leq 0.05$, ** $P \leq 0.01$, *** $P \leq 0.001$, **** $P \leq 0.0001$. Results were presented as mean±S.D. (error bars) of three independent experiments.

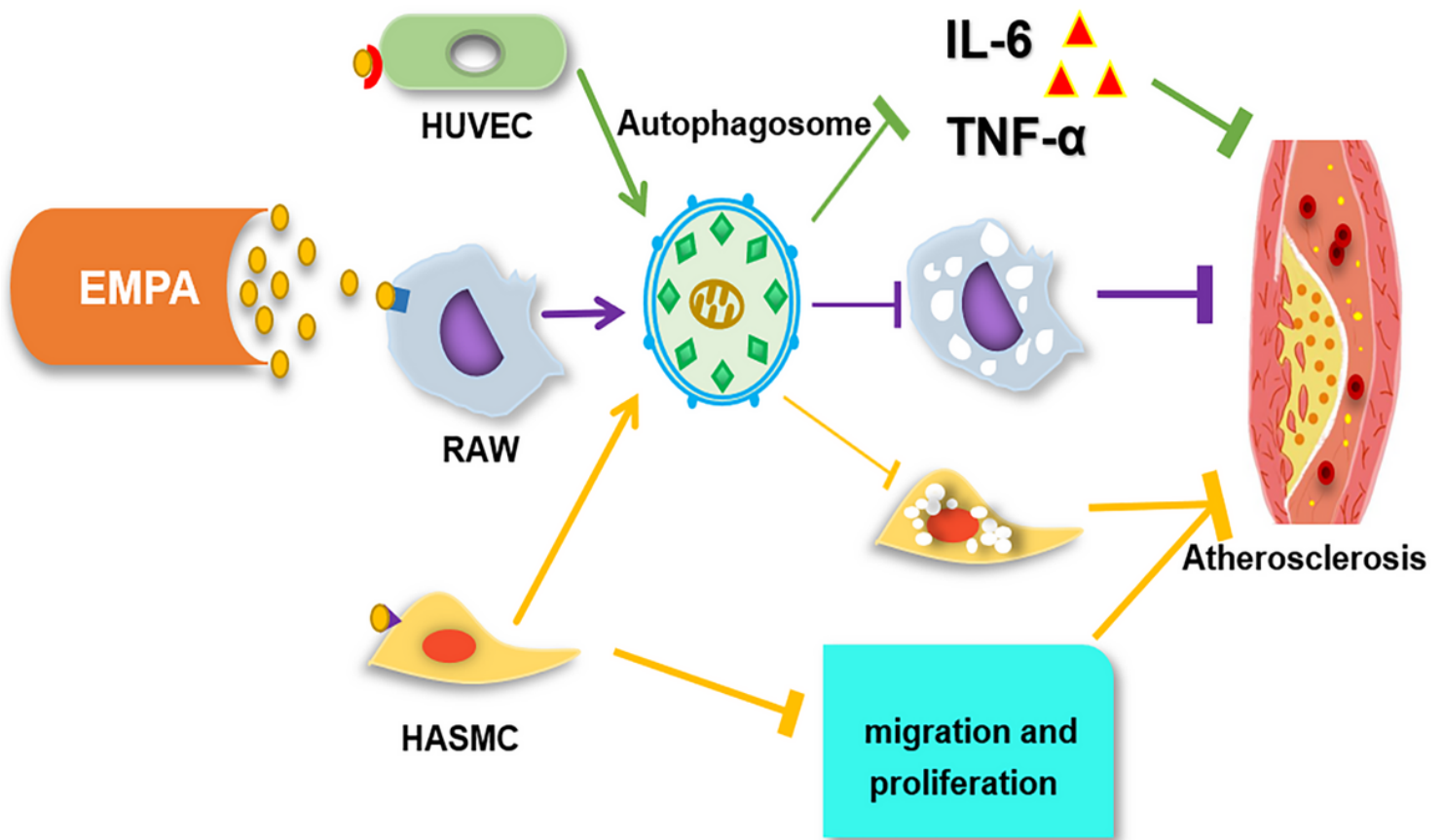


Figure 6

Schematic depiction was about EMPA inhibited atherosclerosis by promoting autophagy. EMPA hindered the formation of macrophage foam cells and the expression of inflammatory factors via autophagy induction in RAW 264.7 cells, thus playing an antiatherosclerotic role. Meanwhile, EMPA prevented the oxLDL-induced inflammatory response in HUVECs by inducing autophagy. Furthermore, EMPA hindered the foaming of HASMCs via autophagy induction as well as the proliferation and migration of HASMCs.